PII: S0032-3861(97)00591-0

Polymer Vol. 39 No. 12, pp. 2557–2561, 1998

0032-3861/98/$19.00+0.00

Effect of physical treatments on the structural organization of a thermotropic polyester

M. Lettieri[a], L. Guadagno[a], V. Vittoria[a,*], G. Galli[b] and E. Chiellini[b]
[a]*Dipartimento di Ingegneria Chimica e Alimentare, Università di Salerno, 84084 Fisciano (SA), Italy*
[b]*Dipartimento di Chimica e Chimica Industriale, Università di Pisa, 56126 Pisa, Italy*
(Received 29 January 1997; revised 21 May 1997)

A main chain liquid crystalline polyester, indicated as LC.10, was quenched into an unoriented nematic state, and crystallized either thermally or with solvents. The different samples were analyzed by X-rays, differential scanning calorimetry, scanning electron microscopy, and transport properties of dichloromethane vapours at different activities. All the results show that both thermal and solvent treatments induce crystallization, but they transform the nematic phase in profoundly different ways. Thermal crystallization transforms the nematic phase into a crystalline phase, leaving unchanged the uncrystallized part. By contrast, the process of solvent-induced crystallization transforms a part of the nematic phase into the crystalline phase, leaving the remaining part in a more disordered phase, resembling the amorphous phase. These different organizations result in very different transport properties of the materials.

(Keywords: liquid crystalline polyester; thermal crystallization; transport properties)

INTRODUCTION

In recent years, polyesters having rigid aromatic mesogens in combination with flexible aliphatic spacers have been extensively synthesized and studied, in order to develop more easily processable thermotropic polymers. This class of polymers shows complex liquid crystalline behaviour and correlations between structure and properties[1–5].

Furthermore, due to the possibility of changing the molecular spacers, the physical properties, and particularly the thermal properties, can be dramatically modified. The spacer length also plays a significant part in determining the relationships between thermomechanical histories and the structural and morphological organization of the samples[6] which, in turn, can be reflected in widely different permeability properties of gases and vapours in films derived therefrom[7–10]. Separation processes or permeability of films used as packaging materials are presently the focus of great interest for their numerous technological implications[11–17].

This paper is a part of a wider study, investigating the influence of flexible spacers on the structural organization of main chain liquid crystalline polyesters, containing an aromatic ester triad as the mesogenic group, and a methylenic segment of different length as the flexible spacer. We have previously analyzed the structural organization and corresponding physical properties of a polymer, consisting of the following repeat unit, after various treatments:

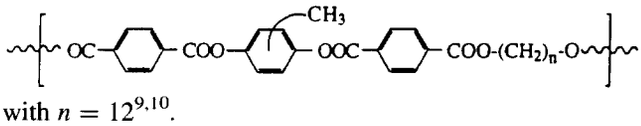

with $n = 12$[9,10].

In this paper we analyze a new homologous polymer, indicated as LC.10, in which $n = 10$.

The main purpose of this work was to study the structure–property relationships for this system, following different thermal and mechanical treatments. The final aim is the determination of the effect of spacer length on the behaviour of these liquid crystalline polyesters.

EXPERIMENTAL

Synthesis

Polyester LC.10 was prepared by the direct polycondensation of a diacid, 1,10-bis-[4-(carboxy)benzoyloxy]decane, and a diphenol, 2-methyl-1,4-hydroquinone, in pyridine solution in the presence of dimethylformamide as an activator and *p*-tosyl chloride as a condensing agent[18]. The crude product was washed with 5% HCl, water and methanol, extracted in a Kumagawa extractor with boiling chloroform and finally precipitated into methanol. It has an average molecular weight $M_w = 66\,000$ (by light scattering) and $M_w/M_n = 2.8$ (by SEC).

Materials

Films of polymer LC.10 were obtained by pressure moulding of the isotropic melt at 240°C and rapid quenching to 0°C in an ice–water bath (sample Q0).

Sample Q0 was either annealed for 3 h at 140°C (sample A140) or immersed in liquid dichloromethane for 24 h, and then dried under vacuum for 24 h (sample S). The recovery of the initial weight and the thermogravimetric analysis demonstrated that sample S was a dry sample, free of solvent molecules. Sample Q was drawn in a dynamometric cell at 60°C up to a draw ratio of 400% (sample D).

Techniques

The thermal behaviour was analyzed by differential scanning calorimetry (DSC) using a Mettler TA 3000

* To whom correspondence should be addressed

calorimeter purged with nitrogen in the temperature range 0–260°C, with a scanning rate of 20°C/min.

Wide-angle X-ray diffraction (WAXD) patterns were obtained using a PW 1710 Philips powder diffractometer (Cu-Kα Ni filtered radiation). The scan rate was 2°C/min.

Scanning electron microscopy (SEM) was carried out using a Stereoscan 90 microscope (Cambridge Instruments, UK). Sections of the samples, obtained by fracture of the film in liquid nitrogen, and treated with a metal sputtering, were analyzed. The thickness of the metal, covering the fracture surface, was 25 nm.

Transport properties were investigated by a microgravimetric method at 25°C, using a quartz spring balance, having an extension of 1.6 cm/mg, according to a previously reported procedure[9]. The permeant was dichloromethane. Sorption was measured as a function of vapor activity $a = p/p_0$ where p is the actual pressure of the experiment, and p_0 the saturation pressure at 25°C.

RESULTS

Wide-angle X-ray diffraction (WAXD)

The WAXD patterns of samples Q0, A140 and S are shown in *Figure 1*. Sample Q0 shows only two peaks, one at $2\vartheta = 9.16°$, and the other, much more intense, at 19.95°. This diffractogram is typical of a quenched nematic phase. Annealing at 140°C transforms part of the nematic phase into a crystalline phase in sample A140, showing the most intense peaks at 15.78, 16.74, 18.41, 20.05, 21.55, 23.74 and 25.58°. The intensity of the peak at 9.16°, already present in the nematic sample Q0, is also increased. The crystalline peaks appear above those of the nematic phase at 20.5°. The nematic contribution to the diffractogram is indicated on the figure with a dotted line.

The diffractogram of sample S also shows a crystalline sample. The solvent treatment, therefore, also induces crystallization in the nematic sample. The positions of the diffraction angles, and the relative intensities of the peaks appearing at 15.16, 18.02, 19.93, 22.04 and 24.43°, are slightly different from those of the crystallized sample A140. Therefore, the thermal and the solvent-induced crystallizations give rise to crystalline forms weakly differing in the crystalline packing. The crystallization is activated in the two cases by heating or swelling the nematic sample. Both processes enhance molecular mobility up to levels suitable for crystallization, but in the latter case specific solvent–polymer interactions can stabilize different chain conformations and/or crystalline packing, as is well documented for other semicrystalline polymers[19–21]. The crystallization of sample Q0 is, therefore, not unexpected, and a similar phenomenon has already been described for the closely related polyester LC.12, with $n = 12$ in the flexible chain. Instead, a more interesting difference between the two samples can be seen in the non-crystalline contribution to the total diffraction. In the case of sample S, in fact, the crystalline peaks are shifted much less with respect to the baseline, the nematic contribution not being as evident as in the thermally crystallized sample. It has been replaced by a much broader and flatter signal, resembling the amorphous contribution to the diffractogram of a semicrystalline polymer.

In the case of the system with $n = 12$[10] we suggested that the process of solvent-induced crystallization transformed the original nematic phase partially into a crystalline and partially into an amorphous phase, resulting in a system very similar to a semicrystalline polymer. Instead, the thermal crystallization transforms part of the nematic phase into a crystalline phase, but leaves the uncrystallized part unchanged. The present system behaves in a similar way, and we can suggest the same explanation to account for the different structures of the crystallized samples.

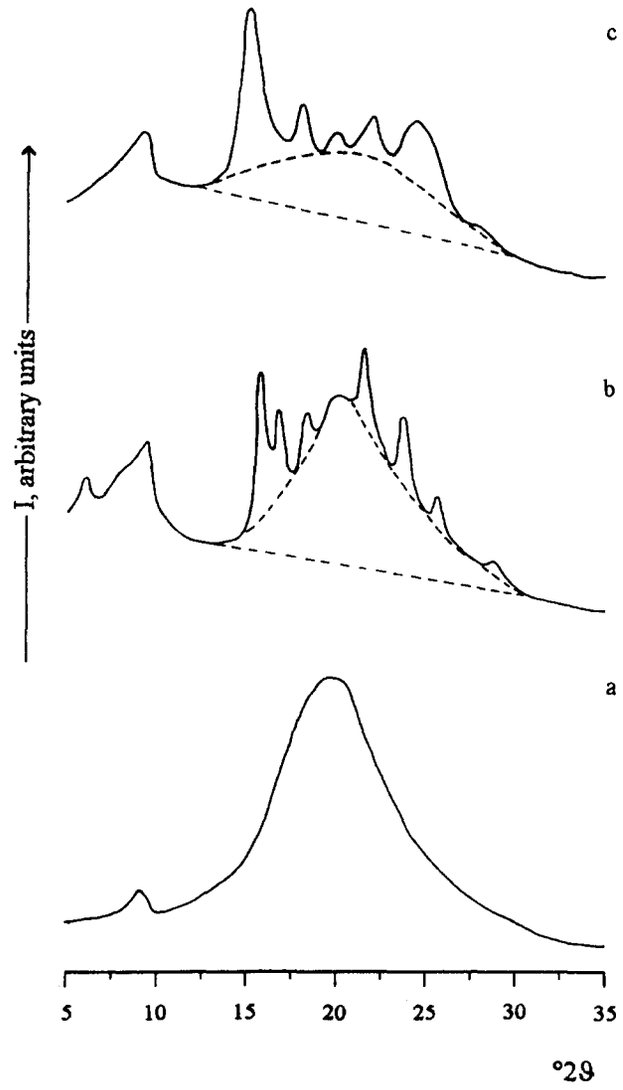

Figure 1 Wide-angle X-ray diffractograms of samples Q0 (a), A140 (b) and S (c)

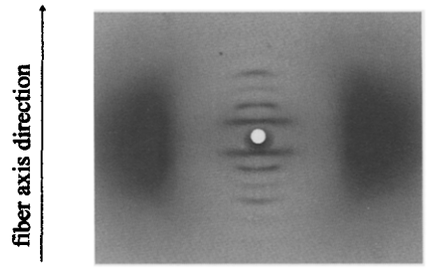

Figure 2 X-ray diffraction pattern of sample D

The WAXD photographic record of sample D is reported in *Figure 2*. A strong polarization of the nematic reflection indicates that the drawing oriented the nematic phase, with the polymer domains being nearly parallel to the drawing direction. Furthermore, the presence of some polarized reflections at lower angles indicates that there is a partial

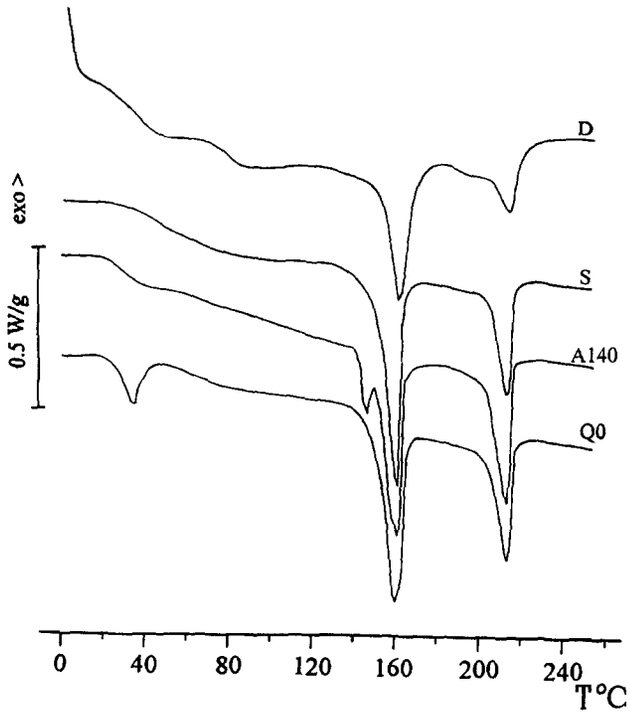

Figure 3 DSC heating curves of samples Q0, A140, S and D, at 20 K/min

lateral correlation between the chains, probably due to an incipient crystallization.

Thermal analysis

The DSC heating traces of the various samples are shown in *Figure 3*. The behaviour in the melting region and in the subsequent isotropization transition is substantially the same in all the samples. Melting and isotropization temperatures (T_m, T_i), as well as the corresponding enthalpies (ΔH_m, ΔH_i) are reported in *Table 1*.

A melt peak is centered at 158.7°C in sample Q0, which shows that the sample crystallized during the heating run. An analogous behaviour is observed for sample D.

In all the treated samples T_m is slightly higher than that of the starting sample Q0, being about 160°C. However, T_i is the same for all the samples. Appreciable differences can be observed below the melting region. Sample Q0 shows an endothermic peak at T_g, which could also be interpreted as the glass transition followed by the exotherm of crystallization. In sample A140 the glass transition is evident at 35°C, very close to that of the starting sample (34°C), whereas the glass transition of sample S is broader and shifted to a higher temperature (45°C). Sample D shows two glass transitions, the first at 34°C, coincident to that of sample Q0, and the other at a higher temperature, 76°C, possibly due to the oriented phase. The location and the origin of the glass transitions in these systems will be the subject of a forthcoming paper.

The exotherm of crystallization of sample D is hardly evident, although a very broad signal can be recognized after the second glass transition. The presence of the orientation modifies the thermodynamics and the kinetics of the crystallization process, justifying a different behaviour compared to sample Q0.

Table 1 Melting (m) and isotropization (i) temperatures and enthalpies, by DSC at 20 K/min heating rate

Sample	T_m(°C)	ΔH_m(J/g)	T_i(°C)	ΔH_i(J/g)
Q0	158.7	16.4	212.2	8.9
A140	160.6	16.4	212.7	8.9
S	160.2	19.5	212.5	9.2
D	160.7	19.8	212.9	7.0

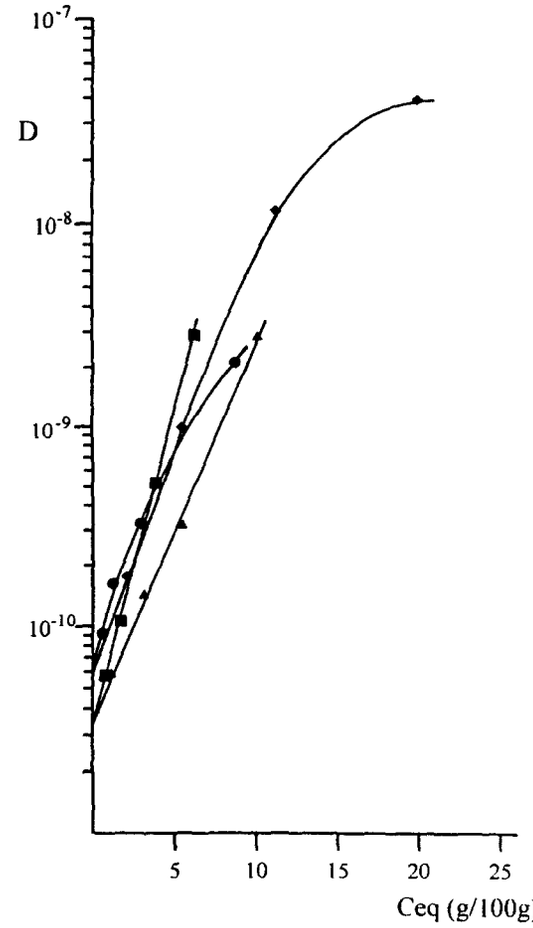

Figure 4 Diffusion coefficient D as a function of equilibrium concentration ceq for samples Q0 (●), A140 (■), D (▲) and S (◆)

Transport properties

In a system composed of phases of different permeabilities, the transport properties show very complex characteristics. However, when one of the phases is impermeable to the penetrant, or shows a much lower permeability, one assumes that all the transport is due to the permeable phase. This phase is presumed to have the same specific sorption capability, irrespective of the extent of the impermeable phase. By increasing the fraction of impermeable phase, there is a decrease of sorption, due to a decreased permeable phase, and, in some cases, a decrease of the diffusion coefficient, due to a more tortuous path for the molecules that must bypass impenetrable crystallites[22].

Diffusion depends on concentration, C_{eq}, at a given activity, and generally this dependence can be expressed as:

$$D = D_0 \exp(\gamma C_{eq}) \quad (1)$$

where D_0 is the zero concentration diffusion coefficient and γ the concentration coefficient. The equilibrium concentration, C_{eq}, is directly related to the fraction of permeable phase[22].

The diffusion coefficient as a function of the equilibrium concentration is given for all the analyzed samples in *Figure 4*. A linear dependence of log D on the concentration

Table 2 Zero concentration diffusion coefficient, D_0, concentration coefficient, γ, and equilibrium sorption, C_{eq}, at vapour activity $a = 0.2$, for all the samples

Sample	$D_0 \times 10^{11}$(cm^2/s)	γ	C_{eq}(g/100g)
Q0	6.25	64	0.58
A140	3.40	65	0.74
S	6.00	51	2.11
D	3.40	44	1.14

is observable, allowing the extrapolation of a D_0 parameter, which can be related to the thermodynamic state of the permeable phase. The γ coefficients were also determined. All the numerical values are reported in *Table 2*. The values of D_0 vary over a small range, between 6.25×10^{-11} cm^2/s for sample Q0, and 3.40×10^{-11} cm^2/s for samples A140 and D.

Such small differences in the D_0 values can be attributed to different tortuosity of the diffusion paths, and not to a different thermodynamic state of the permeable component. The γ coefficient, which is related to the fractional free volume and to the effectiveness with which the solvent plasticizes the polymer, is also very similar for all the samples ($\gamma = 44 \div 65$), confirming that the permeable phase is the same in the differently treated samples. Therefore we conclude that the permeable phase is the amorphous phase and the liquid crystalline phase is impermeable at low activities.

Sorption

In *Figure 5* we report the equilibrium concentration of vapour as a function of the activity for all the samples.

At low activities ($a < 0.4$) quenched sample Q0 and the thermally crystallized sample A140 show a very similar sorption which increases in samples D and S. We deduce

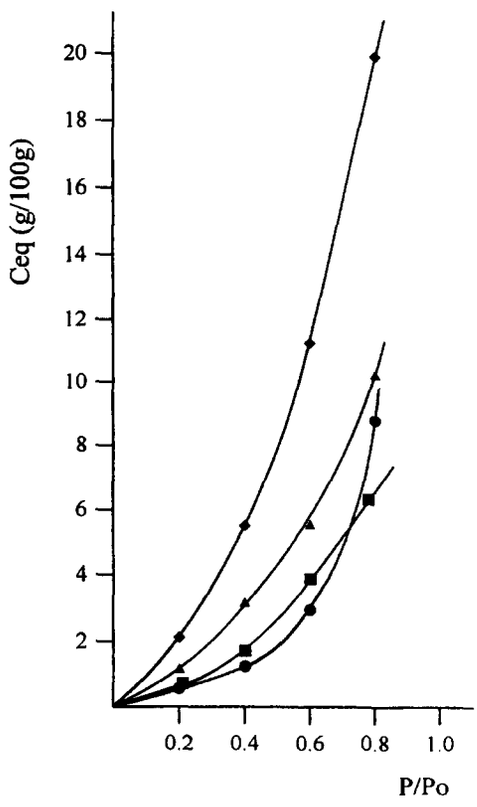

Figure 5 Equilibrium concentration of vapour, C_{eq}, as a function of activity $a = p/p_0$ for samples Q0 (●), A140 (■), D (▲) and S (◆)

that the thermal crystallization of sample A140 transformed a part of the nematic phase into a crystalline phase, leaving the remaining part unchanged. Starting from a two-phase amorphous–nematic system, in which the nematic phase was impermeable at low activities, we obtained a three-phase amorphous–nematic–crystalline system in which the amorphous fraction remained quite similar to that of the starting sample, and the nematic phase became partially crystalline, leaving the total amount of impermeable phase the same as in the starting sample.

This observation is strengthened by observing the behaviour at high activities, where the nematic phase also becomes permeable to the penetrant. At $a > 0.8$ sample Q0 exhibits a much higher sorption with respect to sample A140, in which a part of the nematic phase has become crystalline.

The higher sorption at low activities, observed for sample D, can be explained by an increase in the amorphous fraction, due to the orientation treatment. The process of orienting the nematic domains along the drawing direction leads to a rejection of part of the nematic phase into a more disordered state, i.e. the amorphous phase.

The sorption of sample S is even higher over the entire vapour range. We infer that the solvent-induced crystallization, at variance with the thermal crystallization, completely changes the nematic phase, by transforming part into a crystalline and part into an amorphous phase, the latter being most permeable to the vapours.

Scanning electron microscopy

The SEM photomicrographs of the fracture surface of three of the samples are shown at similar magnifications in *Figure 6*.

Sample Q0 shows a porous structure, in which elongated fibrillar elements are oriented in almost the same direction. Some spherical elements are also observable at the tip of the fibrillar elements. The thermal crystallization does not drastically change this morphology, although the fibrillar structure of the morphological elements becomes more evident.

In the micrograph of sample S spherical elements are present, but in the absence of the elongated elements. They grow on a much smoother surface, resembling an amorphous phase.

DISCUSSION

The LC.10 polyester can be easily quenched into an unoriented nematic state. Both thermal and solvent treatments induce crystallization, but they transform the nematic phase in profoundly different ways.

Thermal crystallization transforms part of the nematic phase into a crystalline phase, leaving the uncrystallized part unchanged, as can be deduced by X-ray and by electron microscopy observations.

The transport properties and the fraction of amorphous phase were not much affected by the thermal treatment. As a result, at high activities sample Q0 absorbs a much larger amount of solvent than sample A140 because, in fact, the nematic phase also becomes permeable to the penetrant.

By contrast, the process of solvent-induced crystallization strongly changes the structural organization of the system, and produces a semicrystalline system. Its morphology does not show oriented elements. Transport properties again indicate that the permeable phase behaves in a similar way, but its fraction has significantly increased.

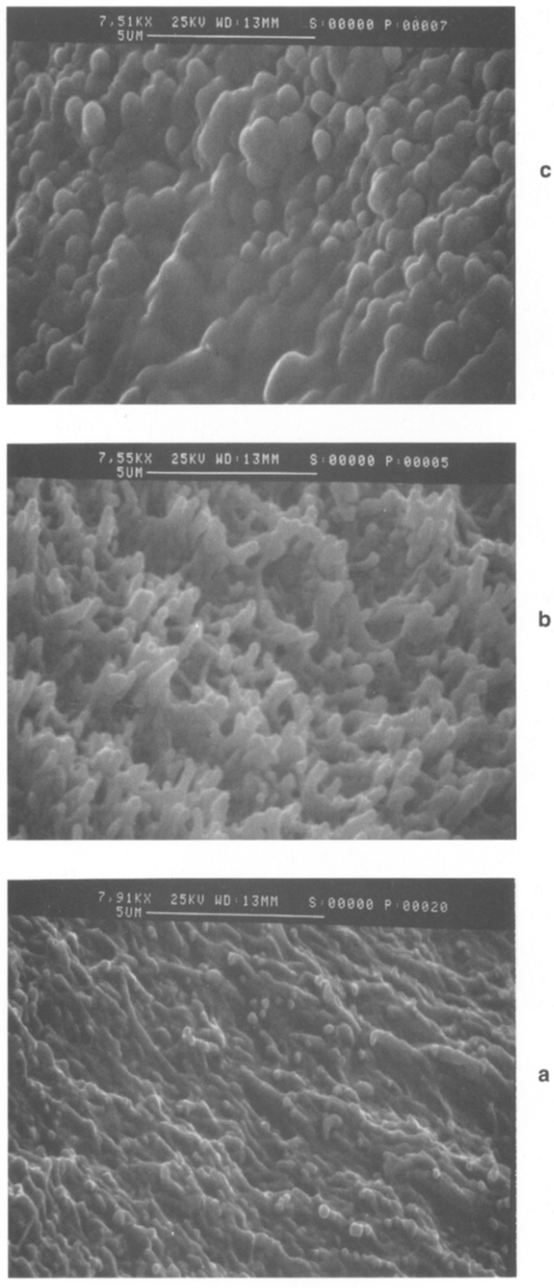

Figure 6 Scanning electron micrographs of the fracture surface of sample Q0 (magnification 7.9 K) (a), A140 (7.55 K) (b) and S (7.51 K) (c)

For example, at activity $a = 0.2$, the sorption increases from 0.58 g/100g for sample Q0 to 2.11 g/100g for sample S. If the specific sorption, C_{sp}, of the amorphous phase is the same in the different samples, we can write:

$$C_{sp} = C_{eq}(Q0)/\alpha a(Q0) = C_{eq}(S)/\alpha a(S)$$

therefore the fraction, αa, of amorphous phase in sample Q0, relative to sample S is:

$$\alpha a(Q0)/\alpha a(S) = 0.27$$

The solvent-induced crystallization occurs through dissolution of the nematic phase, and when solvent evaporation is rapid it can leave the uncrystallized part in a more disordered state with respect to the original nematic phase[23].

The drawing at 60°C does not allow crystallization. However, the orientation of the nematic phase along the drawing direction increases the amorphous fraction, as reflected by an increased sorption at low activities.

In conclusion, while it is possible to quench the nematic phase to room temperature, the three different physical treatments lead to very different structural organizations of the liquid crystalline polymer, comprising nematic, amorphous and crystalline components. These organizations result specifically in very different transport properties of the materials.

REFERENCES

1. Chiellini, E. and Lenz, R. W., in *Comprehensive Polymer Science*, Vol. 5, ed. G. C. Eastmond, A. Ledwith, S. Russo and P. Sigwalt. Pergamon Press, Oxford, 1989, p. 701.
2. Ober, C. K. and Weiss R. A. (eds), *Liquid-crystalline Polymers*. ACS Symposium Series, Washington DC, Vol. 435, 1990.
3. Ciferri, A. (ed.), *Liquid Crystallinity in Polymers*. VCH, New York, 1991.
4. Platè, N. A. (ed.), *Liquid Crystal Polymers*. Plenum Press, New York, 1993.
5. Isayev, A. V., Kyu, T. and Cheng, S. Z. D. (eds), *Liquid Crystalline Polymer Systems*, ACS Symposium Series, Washington DC, Vol. 632, 1996.
6. Frosini, V., de Petris, S., Chiellini, E., Galli, G. and Lenz, R. W., *Mol. Cryst. Liq. Cryst.*, 1983, **223**, 98.
7. de Candia, F., Renzulli, A., Vittoria, V., Roviello, A. and Sirigu, A., *J. Polym. Sci., Polym. Phys. Ed.*, 1990, **28**, 203.
8. de Candia, F., Capodanno, V., Renzulli, A. and Vittoria, V., *J. Appl. Polym. Sci.*, 1991, **42**, 2959.
9. de Candia, F., Guadagno, L., Chiellini, E., Farah, A. A. and Galli, G., *Mater. Sci. Eng.*, 1995, **C3**, 57.
10. Carotenuto, M., Guadagno, L., Vittoria, V., Galli, G. and Chiellini, E., *Macromol. Rapid Commun.*, 1996, **17**, 447.
11. Kajiyama, T., Washizu, S. and Takayanagi, M., *J. Appl. Polym. Sci.*, 1984, **29**, 3955.
12. Chiou, J. S. and Paul, D. R., *J. Polym. Sci., Polym. Phys. Ed.*, 1987, **25**, 1699.
13. Carfagna, C., Amendola, E., Mensitieri, G. and Nicolais, L., *J. Mater. Sci. Lett.*, 1990, **9**, 1280.
14. Modler, H. and Finkelmann, H., *Ber. Bunsenges. Phys. Chem.*, 1990, **94**, 836.
15. Chen, D.-S., Hsiue, C.-H. and Hsu, C.-S., *Makromol. Chem.*, 1992, **193**, 1469.
16. Reinecke, H. and Finkelmann, H., *Makromol. Chem.*, 1992, **193**, 2945.
17. Miranda, N. R., Willis, J. T., Freemann, B. D. and Hopfenberg, H. B., *J. Membrane Sci.*, 1994, **94**, 67.
18. Farah, A. A., Galli, G., Chiellini, E. and Gallot, B., *Polym. J. (Jpn).*, 1994, **26**, 728.
19. Kusuyama, H., Miyamoto, N., Chatani, Y. and Tadokoro, H., *Polym. Commun.*, 1983, **24**, 119.
20. Immirizi, A., de Candia, F., Iannelli, P., Vittoria, V. and Zambelli, A., *Makromol. Chem., Rapid Commun.*, 1988, **9**, 761.
21. Corradini, P. and Guerra, G., *Adv. Polym. Sci.*, 1992, **100**, 183.
22. Peterlin, A., *J. Macromol. Sci. Phys.*, 1975, **B11**, 57.
23. Khattacharya, S. K., Misra, A. and Stein, R. S., *J. Polym. Sci. Phys. Ed.*, 1986, **26**, 515.